Investigations into the impact of bond pads and p-stop implants on the detection efficiency of silicon micro-strip sensors

Luise Poley[1], Kristin Lohwasser[1], Andrew Blue[2], Mathieu Benoit[3], Ingo Bloch[1], Sergio Díez[1], Vitaliy Fadeyev[4], Bruce Gallop[5], Ashley Greenall[6], Ingrid-Maria Gregor[1], John Keller[1], Carlos Lacasta[7], Dzmitry Maneuski[2], Lingxin Meng[3,6], Marko Milovanovic[1], Ian Pape[8], Peter W. Phillips[5], Laura Rehnisch[9], Dennis Sperlich[9], Craig Sawyer[5], Martin Stegler[1], Yoshinobu Unno[10], Matt Warren[11], and Eda Yildirim[1]

[1]Deutsches Elektronen-Synchrotron, Notkestraße, Hamburg, Germany
[2]SUPA School of Physics and Astronomy, University of Glasgow, University Avenue, Glasgow, United Kingdom
[3]Département de Physique Nucléaire et Corpusculaire, University of Geneva, quai Ernest Ansermet, Genève, Suisse
[4]Santa Cruz Institute of Particle Physics, University of California, High Street, Santa Cruz, United States of America
[5]Particle Physics Department, STFC Rutherford Appleton Laboratory, Harwell Science and Innovation Campus, Didcot, United Kingdom
[6]Department of Physics, University of Liverpool, Cambridge Street, Liverpool, United Kingdom
[7]Instituto de Física Corpuscular, CSIC-U. Valencia, c/ Catedrático José Beltrán, Paterna, Spain
[8]Diamond Light Source Ltd, Diamond House, Harwell Science and Innovation Campus, Didcot, United Kingdom
[9]Institut für Physik, Humboldt-Universität zu Berlin, Newtonstraße, Berlin, Germany
[10]Institute of Particle and Nuclear Study, KEK, Oho, Tsukuba, Japan
[11]Department of Physics and Astronomy, University College London, Gower Street, London, United Kingdom

November 21, 2016

Abstract

The High Luminosity Upgrade of the LHC will require the replacement of the Inner Detector of ATLAS with the Inner Tracker (ITk) in order to cope with higher radiation levels and higher track densities. Prototype silicon strip detector modules are currently developed and their performance is studied in both particle test beams and X-ray beams. In previous test beam studies of prototype modules, silicon sensor strips were found to respond in regions varying from the strip pitch of 74.5 µm. The variations have been linked to local features of the sensor architecture.

This paper presents results of detailed sensor measurements in both X-ray and particle beams investigating the impact of sensor features (metal pads and p-stops) on the responding area of a sensor strip.

1 Introduction

In the current layout for silicon strip sensor modules for the future ATLAS Inner Tracker, modules consist of silicon strip sensors, printed circuit boards (hybrids) [1] and binary readout chips (ABC130 ASICs [2]). Readout chips are glued on to hybrids, which are then glued on to sensors. Electrical connections between readout chips and hybrids are made by aluminium wire bonds (diameter 25 µm), providing both power for the chips and data readout connections.

Wire bonds also connect each sensor strip to an ASIC readout channel: the energy deposited in the bulk by a traversing charged particle or absorbed photon is detected in 1-2 silicon strips, providing spatial information corresponding to the pitch of a sensor strip (74.5 µm). Each sensor strip is read out individually by one ASIC channel. The connection of ASICs and sensor strips by wire bonds requires the addition of electrically conductive bond pads to the aluminium layer on top of each strip implant. The dimensions of these bond pads are defined by necessities for safe wire bonding:

- a single bond foot (the area over which a wire bond is connected to a bond pad) has a width and length of up to $35 \times 120\,\mu m^2$ (see figure 1)
- a typical wire bonding wedge used for this application has a width of about 80 µm
- in case of wire bonding failures, further wire bonding attempts can be necessary, requiring a bond pad size sufficient to place two wire bond feet side by side

Consequently, bond pads were chosen to have an approximately rectangular shape of $56 \times 200\,\mu m^2$ (see figure 1), i.e. close to the strip pitch (74.5 µm).

Silicon strip sensors for the ATLAS Inner Tracker consist of a p-doped bulk with n-doped strip implants [3]. In order to electrically separate individual strip implants, p-doped implants (p-stops) are positioned between strip implants. With a strip pitch of 74.5 µm and a bond pad width of 56 µm for safe wire bonding, bond pads need to be positioned in a staggered design of two rows, alternatingly on odd and even numbered sensor strips. P-stop implants, which which for most of the length of strips are straight and at the centre between two neighbour sensor strip impants, are arranged around these bond pads, leading to uneven distances between p-stops and strip implants (see figure 2).

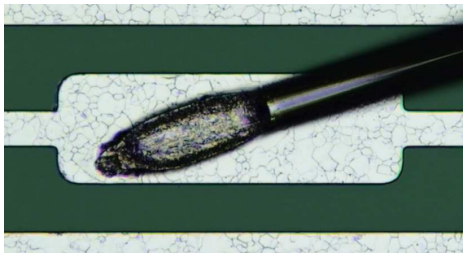

Figure 1: Laser microscope image of a wire bond foot on an aluminium bond pad on a silicon sensor. The bond wire (diameter 25 µm) is pressed down and, by using ultrasonic power, welded on to the bond pad, increasing its width on the bond pad to about 35 µm. The length of the wire bond footprint is about 120 µm. The bond pad is longer than the bond foot to allow repeated wire bonding attempts, i.e. more than one bond foot on the same bond pad.

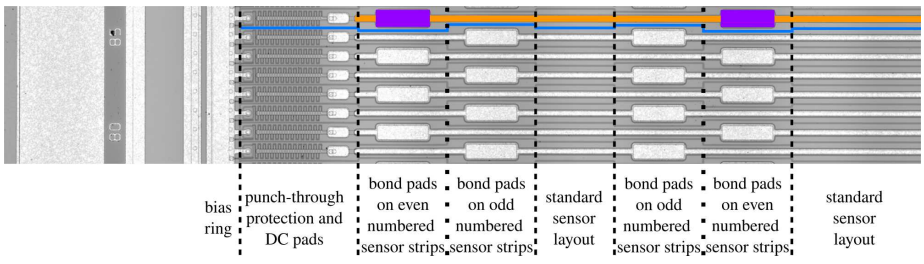

Figure 2: Laser microscope image of a miniature sensor showing bias ring, punch-through protection [4] and sensor strips (orange) with bond pads (violet), electrically separated by p-stop implants (blue). While in the standard sensor layout areas (without bond pads) p-stop implants are straight and have a pitch of 74.5 µm, bond pad rows show p-stop implants arranged around the bond pads, leading to uneven distances between neighbour p-stop implants. One complete row of bond pads, comprised of one row of bond pads on even numbered sensor strips and one row of bond pads on odd numbered strips, stretches over a length of 700 µm.

ATLAS07 [3] and ATLAS12 [5] sensors were produced as realistic prototypes for sensor tests, with a sensor architecture similar to the sensors to be used in the future ATLAS strip tracker.

First indications that sensor strip responses might be different in sensor regions with and without bond pads were found in measurements to investigate charge sharing between adjacent strips [6]. These measurements were conducted at beamline B16 [7] of the Diamond Light Source using a micro-focused X-ray beam with a photon energy of 15 keV (see section 4). Scanning the bond pad area of adjacent silicon sensor strips in an X-ray beam, the responding width of individual sensor strips had been found to match the uneven p-stops positions in that area rather than the strip pitch.

2 Particle test beam measurements

Further measurements were performed using an ATLAS07 miniature sensor prototype [3] with an active area of $\sim 7 \times 7\,\mathrm{mm}^2$. Test beam measurements were performed with the sensor placed inside a beam telescope (described in [8]). The beam telescope consists of six planes of MIMOSA26 pixel sensors, arranged in groups of three in front of and three behind the device under test. A particle passing through the sensor under investigation is also registered in each telescope plane. MIMOSA26 sensor pixels have a pitch of 18.4 µm, allowing the reconstruction of each particle track with high spatial resolution ($\mathcal{O}(\mu\mathrm{m})$) [9].

The tracks of the beam particles traversing the telescope are reconstructed from signal clusters reeconstructed in the telescope planes using the General Broken Lines (GBL) Algorithm [10]. The alignment parameters are calculated using the Millepede-II Algorithm [11].

The charge deposited in the sensor was read out via wire bonds connecting the sensor to the analogue readout system ALiBaVa [12]. The charge collected in each ALiBaVa readout channel is compared to the average expected noise in each channel. The collected charge in the channel with the largest signal-to-noise ratio (SNR), requiring at least a SNR of five, is then further used to form a cluster. The charge collected in adjacent channels is added to the cluster if the SNR in the respective channel exceeds three. The reconstructed clusters are then taken to be hits caused by the traversing particles from the beam. Each hit found by the readout system can be related to a particle track reconstructed in the beam telescope in a given recorded beam event. By investigating which sensor strip responded with a signal and relating this to the expected hit position on the sensor given the parameters of the particle track reconstructed in the beam telescope, the area over which a strip collected signals could be mapped directly in x-y space.

Both the ALiBaVa daughterboard (used for signal readout) and the sensor board (holding the miniature sensors) were mounted on a copper plate cooled down to 10 °C. The cooling plate was mounted inside a plastic housing to minimise light exposure. The sensor was operated fully depleted at a bias voltage of -200 V.

2.1 Results

Figure 3 shows the resulting map of clusters obtained for one ATLAS07 miniature sensor. The number of recorded particle hits per sensor position showed

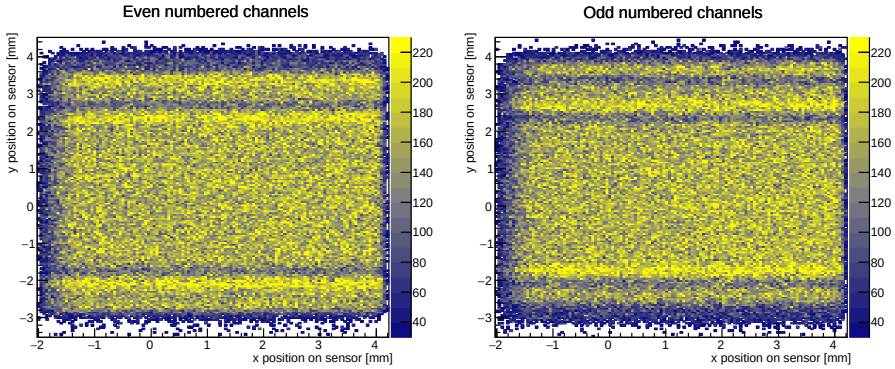

Figure 3: Positions of particle hits on an ATLAS07 miniature sensor for 6 million events. The sensor strip implants are oriented parallel to the y-axis. The left plot shows the hit map of only even numbered sensor strips, the right plot shows the hits collected only by odd numbered strips. Areas with fewer hits are paired with areas with more hits, matching the positions of bond pad rows consisting of one row of bond pads for even numbered channels and one row of bond pads for odd numbered channels each. Both hitmaps show complementary effects (more/fewer events) in the same areas, indicating that the overall number of hits was consistent over the full sensor area, but the distribution between odd and even numbered channels changed in bond pad areas.

that the presence of bond pads leads to a statistical effect on the number of recorded hits: sensor strips with bond pads show an increased number of hits in the bond pad area, while sensor strips without bond pads show fewer hits in the same area. Since the overall number of hits (i.e. the combined hits from odd and even numbered channels) is approximately constant over the whole sensor area, an increased/decreased number of hits indicates hits were collected over a larger/smaller sensor area. Figure 4 shows a projection of the number of collected hits in order to attempt a quantification of the effect. After the previous test beam results had indicated that bond pads might lead to different widths over which a sensor strip responds, the findings from this test beam showed a similar effect: the presence of a bond pad on a sensor strip results in this strip collecting hits over a larger area than intended. This effect leads to an average difference of up to 30 % in collected clusters in bond pad regions compared to sensor regions without bond pads.

The effect was made more visible by dividing the sensor area in a grid with bin sizes of $14.9 \times 149\,\mu\text{m}^2$ and finding the sensor channel collecting the most hits for any given position. Figure 5a shows the resulting response map for an ATLAS07 miniature sensor in comparison with its bond pad layout (see figure 5b). The hit map confirms that the modified sensor architecture in bond pad areas affects the area over which a sensor strip collects charges: a sensor strip responds in a wider area around a sensor bond pad, while neighbour sensor

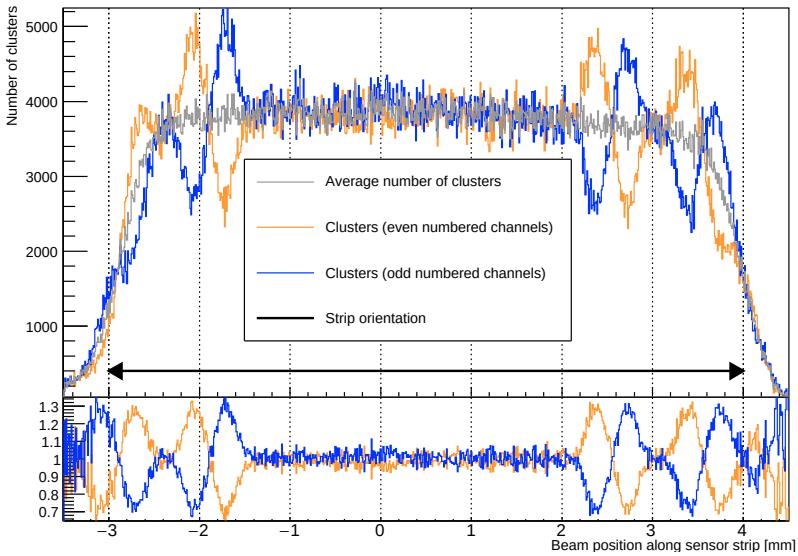

Figure 4: 6 million hits collected on an ATLAS07 miniature sensor, projected on on the sensor axis parallel to the strip implants. Separating the clusters according to the highest responding channel (odd/even) shows regions where the number of clusters in odd/even channels deviates from the average by up to 30 %. The variations of clusters collected in odd/even numbered channels complement one another, indicating that the cluster distribution has changed, not the overall efficiency. The pattern of more/fewer clusters matches the positions of bond pad rows on the sensor.

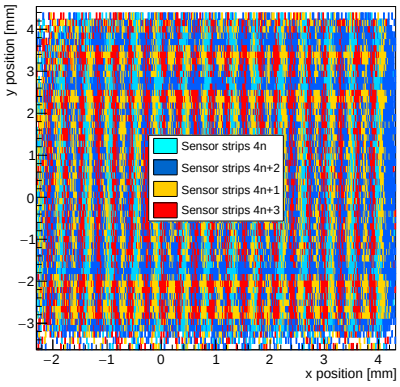

(a) ATLAS07 miniature sensor map showing the mainly responding sensor strip for a given position on the sensor: orange and red bins represent odd numbered channels, cyan and blue bins represent even numbered channels.

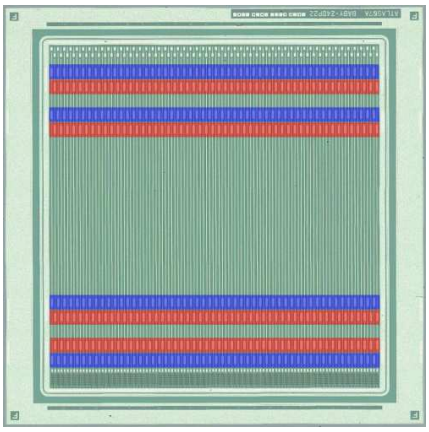

(b) ATLAS07 miniature sensor in the same orientation as used in the test beam. Bond pads of odd and even numbered channels are colored red and blue, with a total of eight rows of bond pads on the miniature sensor.

Figure 5: Sensor hit map in comparison with the sensor layout: the size of the hitmap has been scaled to approximately match the active area of the miniature sensor. The hit map shows that in several areas of the sensor the mainly responding channels are almost exclusively odd or even. The positions of these areas match the bond pad rows indicated on the sensor layout. It can be seen that the pattern of bond pad rows (alternating on even and odd channels in the sensor top half, even-odd-odd-even in the bottom half) is also found in the pattern of mainly responding channels, indicating that the effect found in the hit map is caused by the array of bond pad rows on the sensor.

strips respond over a smaller area.

The effect of sensor strips responding over smaller or wider areas than expected could not be unambiguously attributed to either the presence of bond pads or modified p-stop positions, given the maximum resolution achieved with the telescope in the setup.

3 Sensor layout considerations

The ATLAS12 [5] sensor is divided in four strip segments, where each segment has a length of $\sim 2.5\,\mathrm{cm}$ and five rows of bond pads. Each row, consisting of bond pads on odd and even numbered sensor strips, accounts for $700\,\mu\mathrm{m}$ of modified p-stop positions of which bond pads make up $400\,\mu\mathrm{m}$. With overall dimensions of $9.75 \times 9.75\,\mathrm{cm}^2$, five rows of bond pads on each of the four strip segmentes lead to a total of 14 mm (14.4 %) of modified p-stops and 8 mm (8.2 %) of bond pads on one sensor strip.

In these areas, charge collection differs from the expected standard sensor behaviour and thus particle tracking can be affected. Depending on the main contributor to the variations (modified p-stop positions or bond pads), a modification of the sensor layout could be contemplated:

- if bond pads were found to affect the responding area of a sensor strip, the number of bond pad rows on the sensor could be reduced
- if modified p-stop positions were found to define the area over which a strip responds, the sensor architecture could be modified (using optimised p-stop positions or a sensor architecture with p-spray) or a track reconstruction algorithm including position information associated with the sensitive sensor regions could be implemented

In order to identify the mainly defining element of a sensor strip's responding area, a further study with high positioning precision was performed.

4 Mapping in an X-ray beam

In order to investigate the impact of p-stops and bond pads on the charge collecting area of a sensor strip, a micro-focused X-ray beam ($2 \times 3\,\mu\mathrm{m}^2$, see figure 6) was used. The sensor was moved in the beam to scan different areas of the sensor (see figure 7) in order to compare any potential differences to how sensor strips responded with X-ray focused on various sensor architectures including:

- equidistant p-stops
- modified p-stop positions
- modified p-stop positions around bond pads

By using a beam size much smaller than the structures under investigation, differences in the number of collected hits for different sensor areas can be resolved. Also, the position of the beam with respect to the sensor is very well known.

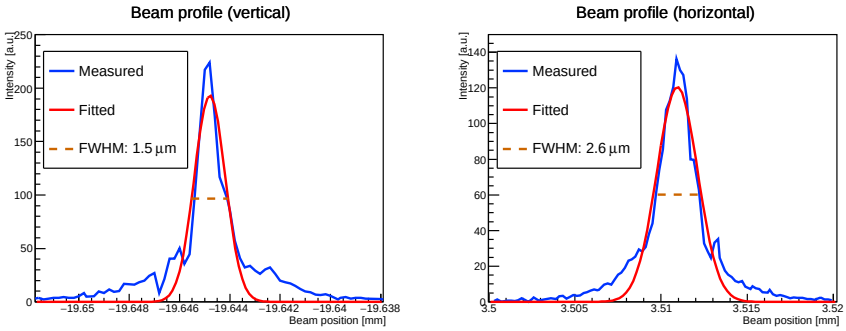

Figure 6: X-ray beam profiles measured using by inserting a gold wire: the horizontal and vertical beam width were measured to be 1.5 µm and 2.6 µm.

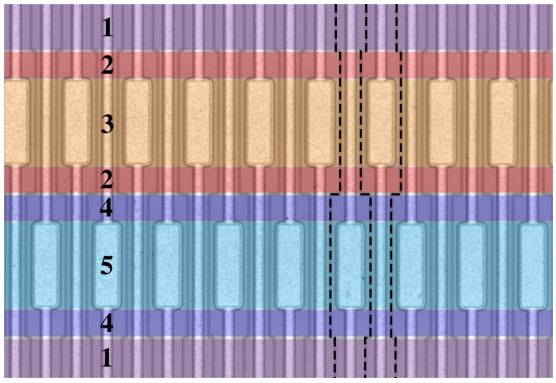

Figure 7: Laser microscope image of bond pad rows on sensor showing the different sensor architectures around bond pads. P-stops are visible as dark lines between strip implants with aluminium tops and bond pads. The standard sensor layout with equidistant p-stops is coloured violet (1). Bond pads on odd (light blue, 5) and even (orange, 3) numbered strips show different p-stop positions (dashed black lines), arranged around the bond pads. Between bond pads and standard sensor layout, a transition region (red (2)/dark blue (4)) can be seen, where p-stops are not equidistant, but no bond pads are present.

	x-direction (across sensor strips), [µm]	y-direction (along sensor strips), [µm]
bond pad	60	200
modified p-stops		
around bond pads	52	350
between bond pads	97	350
scanning step	15	60
scanning length	210	open

Table 1: Parameters of a grid scan over the bond pad area of an ATLAS07 sensor: step sizes were chosen to be smaller than sensor architecture features.

4.1 Setup

The effect was studied for two devices in comparison:

- a non-irradiated ATLAS12 [5] miniature sensor, attached to an ABC130 readout chip, using the same setup as used in the initial measurements [6], where an effect was first observed
- one irradiated ATLAS07 miniature sensor (irradiated with reactor neutrons to $2 \cdot 10^{15}\,\mathrm{n_{eq}/cm^2}$, connected to an ALiBaVa readout system, using the same test beam setup as in the DESY test beam (see section 2)

An ATLAS07 sensor with the same geometry as the ATLAS12 sensor was chosen for comparability. In the case of p-stops defining the area over which a sensor strip responds, any effect was predicted to increase after irradiation. Hence, two sensors of the same architecture, one irradiated and one non-irradiated, were tested.

While the different readout systems connected to the two sensors required different modes of data taking concerning the number of triggers and collected hits, the gemoetrical parameters of scans on both sensors were chosen to be identical (see table 1). The scan length perpendicular to the strip orientation was chosen to ensure that one strip was entirely covered, including its presumably widest area around its bond pad. Step sizes were chosen to ensure that at least one point of the scanning grid would fall into each of the sensor architectures of interest, in particular the region where p-stops were not equidistant, but no bond pads were present (indicated in figure 7).

For the irradiated sensor read out by an ALiBaVa system, 100 000 events were collected for each position of the beam on the sensor (trigger rate 25 ns). For the non-irradiated sensor attached to an ABC130 readout chip, a threshold scan was performed for thresholds ranging from 62 mV to 152 mV (see figure 8). For each beam position, 10 000 triggers per threshold were sent to each readout channel. For each trigger, a hit was registered in a channel if its collected charge exceeded the preset threshold.

4.2 Results

For each sensor strip covered in the scan, the collected hits for each beam position were plotted to map its responding area. Figure 9 shows the scanned

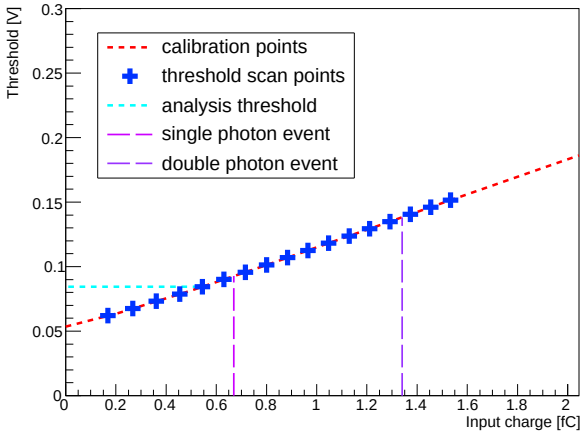

Figure 8: Thresholds and input charges for an ABC130 readot chip connected to an ATLAS12 sensor: the thresholds corresponding to any given input charge were calculated using internal calibration circuits of the readout chips. The threshold corresponding to the expected input charge of a 15 keV electron, 0.67 fC, was found to correspond to a threshold of 93 mV. For data taking, a lower readout threshold of 85 mV was chosen.

sensor area and the corresponding hit maps. The results show that the width over which a sensor strip responds does depend on the sensor architecture at that position: the presence of bond pads increases the area over which a sensor responds, with the number of hits collected by neighbour strips decreasing accordingly.

In order to investigate the impact of p-stop positions on the responding sensor area, sensor areas without bond pads but with non-uniform p-stop positions were studied. Analogous to the map shown in figure 5a, the number of hits collected in each channel was compared for each bin, showing the highest responding channel for each beam position. Figure 10 shows the resulting sensor map. It was found that strip sensors responding over wider or narrower areas can be attributed mainly to the presence of bond pads, with the p-stop positions having only a minor impact. These results are qualitatively consistent with TCAD simulation studies which varied the strip implant widths and p-stop positions.

Irradiation was suspected to influence the electric field of the sensor and thus the responding area of each sensor strip. The results obtained for a non-irradiated sensor were compared to a similar scan performed to an ATLAS07 sensor irradiated to a fluence of $2 \cdot 10^{15}$ 1 MeV neutrons/cm^2 using reactor neutrons. This corresponds to the full High Luminosity LHC dose expected in the ATLAS strip tracker, including a safety factor of 2. Figure 11 shows the hit maps obtained from individual sensor strips of an irradiated sensor. The hit maps for sensor strips on an irradiated sensor were found to agree with the results of the non-irradiated sensor. Both sensors did showed only small impacts of different p-stop positions on the responding area of a sensor strip, while the presence of bond pads on sensor strips did increase the responding width of the

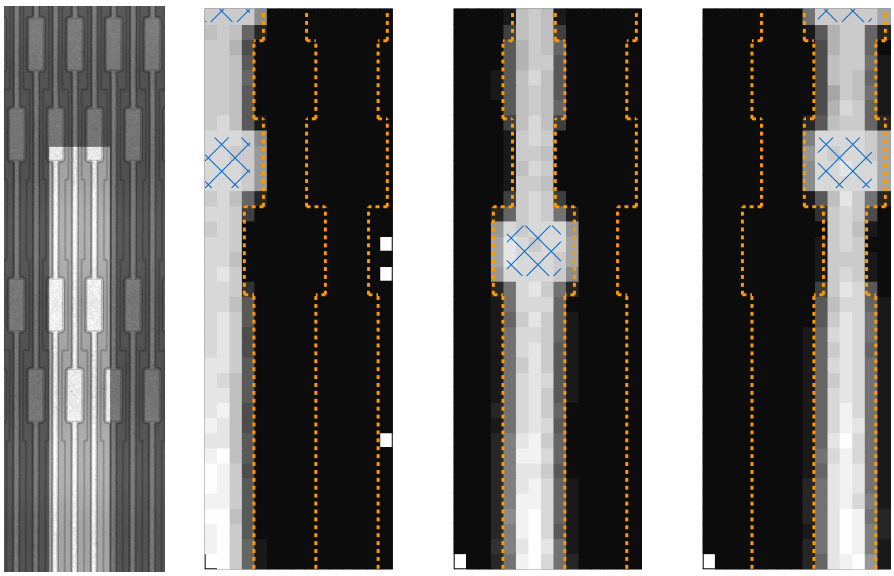

Figure 9: Laser microscope image of the approximate sensor area (highlighted) covered in X-ray beam scan (left) and resulting three hit maps (right). Each plot shows the signals collected by one readout channel for the same scan area of $2.1 \times 0.21\,\mathrm{mm}^2$. Hits were collected over a grid scan in steps of $15 \times 60\,\mu\mathrm{m}^2$. Numbers of hits were scaled relative to the maximum number of hits for comparability between channels. Positions of p-stops (dashed orange lines) and bond pads (blue shaded areas), determined from fits of cllected hit distributions, are indicated on the hit maps. The hit maps show the sensor strips responding over a wider area around bond pads and correspondingly narrower areas between bond pads on neighbour sensor strips.

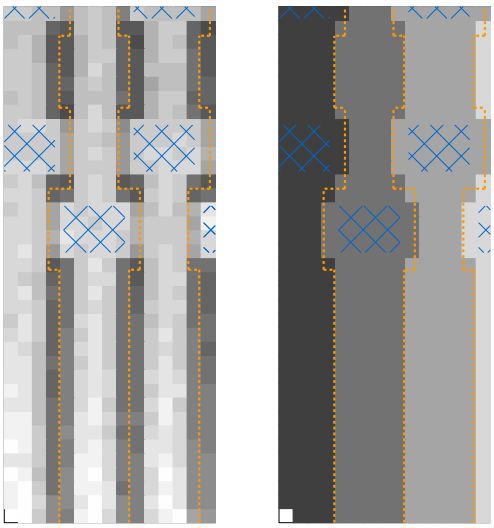

Figure 10: Combined hits from four adjacent sensor strips over a $2.1 \times 0.21\,\mathrm{mm}^2$ area of a sensor bond pad region. Combined hits from neighbour channels (left image) show that, around bond pads, the number of collected hits is higher than in the standard sensor area without bond pads. Mapping the mainly responding channel for each beam position (right image) shows that the area over which a sensor strip responds does not follow the shape of a p-stop: sensor strips show similar responses in areas with equidistant and unevenly spaced p-stops.

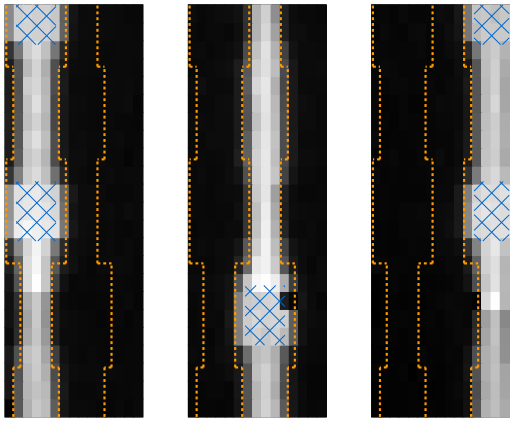

Figure 11: Hit maps for three sensor strips over an area of $1.32 \times 0.21\,\mathrm{mm}^2$ in steps of $60 \times 15\,\mu\mathrm{m}^2$. Hit numbers are shown relative to the maximum number of hits collected for one sensor strip. Positions of sensor features (p-stops (dashed orange lines) and bond pads (shaded blue areas)) were determined from hit distributions and are shown on the maps. While the responding areas of individual strips are larger around bond pads, no difference could be observed between areas with equidistant p-stops and unevenly spaced p-stops.

strip while reducing the responding width for the neighbour channels next to the bond pads.

It should be noted that the number of photons passing through the sensor for each beam position was found to vary over time, translating into different numbers of hits being collected. Figure 11 shows a visible discrepancy in collected hits between two areas on the hit map, with the transition being marked by one bin showing significantly fewer entries than the surrounding positions. Comparing the timestamps of each beam position with the beam current, changes over time were found to match the variations observed in the numbers of collected hits. Figure 12 shows the measured beam current over time. The hit map entry with the low number of entries was found to correspond to a beam loss, leading to a low number of photons and registered hits. After restarting, the beam current was higher than before and slowly decreasing, translating into the same effect on the obtained hit map. While the changes of the beam current complicate absolute statements about collected hits and efficiency, the variations were small enough to allow for the comparison of responding sensor areas.

5 Conclusion and Outlook

Studies of the bond pad regions of silicon strip sensors with high spatial resolution have confirmed that on ATLAS07 and ATLAS12 sensors, strips respond over a larger width when bond pads are present. It was found that the strip response can be attributed mainly to the geometry of bond pads, with the impact

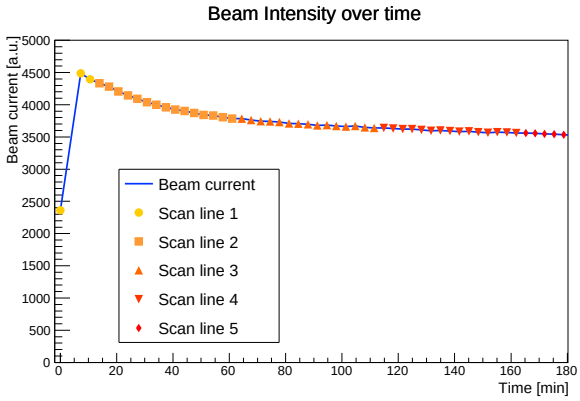

Figure 12: Beam line current measured after a restart. Each marker represents one beam position of the scan grid, with one scan line consisting of 15 scan points across the sensor strips. The beam current decreases by 22 % over three hours, corresponding to five scanning lines, but stays comparably stable across one scan line.

of p-stop positions being much smaller.

Bond pads were found to increase the local width over which a sensor strip collects hits from 74.5 µm to $\sim$ 95 µm and reduce the responding width of adjacent strips to $\sim$ 54 µm. Estimating from the number of collected clusters in different sensor areas, the wider/narrower signal collecting widths translate into up to 30 % more/fewer signals collected in these areas. Comparable effects can be assumed to occur in sensors with similar architecture features.

Detector simulation studies will be conducted in order to investigate the potential impact of effective strip widths varying along the strip length on the tracking performance. Significant negative impacts on the tracking performance could be the base for modifications of the final sensor layout.

Acknowledgements

The measurements leading to these results have been performed at the Test Beam Facility at DESY Hamburg (Germany), a member of the Helmholtz Association (HGF). We thank the test beam coordinators and telescope support, Dr. Marcel Stanitzki and Dr. Jan Dreyling-Eschweiler in particular, for their help and support during the test beam.

We thank Diamond Light Source for access to beamline B16 (proposal number MT13500) that contributed to the results presented here, especially Dr. Kawal Sawhney for his help with the setup and his support throughout our measurement. The authors would like to thank personnel of the B16 beam, especially Andy Malandain, for providing advice, support and maintenance during the experiment.

This project has received funding from the European Union's Horizon 2020 Research and Innovation programme under Grant Agreement no. 654168. The authors would like to thank Dr. Vladimir Cindro from JSI for his help with the sensor irradiations.

The work at SCIPP was supported by the Department of Energy, grant DEFG02-13ER41983.

References

[1] V. Benitez et al. Development and investigation of hybrids and modules for the Phase-II Upgrade of the forward region of the silicon strip tracking detector of the ATLAS experiment. to be submitted to Journal of Instrumentation.

[2] T Affolder et al. System Electronics for the ATLAS Upgraded Strip Detector. Technical Report ATL-UPGRADE-PUB-2013-011, CERN, Geneva, Feb 2013.

[3] Y. Unno et al. Development of n-on-p silicon sensors for very high radiation environments. *Nuclear Instruments and Methods in Physics Research Section A: Accelerators, Spectrometers, Detectors and Associated Equipment*, 636(1, Supplement):S24 – S30, 2011. 7th International Hiroshima Symposium on the Development and Application of Semiconductor Tracking Detectors.

[4] K. Hara et al. Design of Punch-Through Protection of Silicon Microstrip Detector against Accelerator Beam Splash. *Physics Procedia*, 37:838 – 843, 2012.

[5] Y. Unno et al. Development of n+-in-p large-area silicon microstrip sensors for very high radiation environments – ATLAS12 design and initial results. *Nuclear Instruments and Methods in Physics Research Section A: Accelerators, Spectrometers, Detectors and Associated Equipment*, 765:80 – 90, 2014. HSTD-9 2013 - Proceedings of the 9th International Hiroshima Symposium on Development and Application of Semiconductor Tracking Detectors International Conference Center.

[6] Luise Poley et al. Characterisation of strip silicon detectors for the ATLAS Phase-II Upgrade with a micro-focused X-ray beam. *Journal of Instrumentation*, 11(07):P07023, 2016.

[7] K. J. S. Sawhney et al. A test beamline on diamond light source. *AIP Conference Proceedings*, 1234(1):387–390, 2010.

[8] Jansen, Hendrik et al. Performance of the EUDET-type beam telescopes. *EPJ Techn Instrum*, 3(1):7, 2016.

[9] Igor Rubinskiy and Hanno Perrey. An EUDET/AIDA Pixel Beam Telescope for Detector Development. *PoS*, TIPP2014:122, 2014.

[10] C. Kleinwort. General Broken Lines as advanced track fitting method. *Nuclear instruments & methods in physics research A*, 673:107–110, 2012.

[11] V. Blobel. Software alignment for tracking detectors. *Nucl. Instrum. Meth.*, A566:5–13, 2006.

[12] ALiBaVa systems. *ALiBaVa: A startup guide*.

This figure "Sensorim.png" is available in "png" format from:

http://arxiv.org/ps/1611.06114v1